Eur. Phys. J. D **9**, 535–538 (1999)

THE EUROPEAN PHYSICAL JOURNAL D

EDP Sciences

In situ observation of coalescence growth of small gold clusters by X-ray diffraction technique

K. Koga[a,b] and H. Takeo[a]

National Institute for Advanced Interdisciplinary Research, Tsukuba, Ibaraki 305-8562, Japan

Received: 1 September 1998 / Received in final form: 20 October 1998

Abstract. An *in situ* observation of coalescence growth among small Au clusters (1–2 nm) have been performed by means of a grazing-incidence X-ray diffraction method. The Au clusters, having predominantly the decahedral multiple-twinned structures, were piled up on a cold Si substrate at 92 K so that the coalescence growth could be avoided. By annealing the sample from 82 K up to 325 K, the broad diffraction pattern was found to be gradually sharpened as the annealing temperature increased. The morphology was observed by scanning electron microscopy, after annealing at 325 K showed lumpy-type networks having a typical lump size of 100 nm, indicating coagulation growth of clusters. However, the corresponding diffraction pattern could not be explained without the multiple-twinning relation of small grains; this suggests that the initial cluster structure strongly influences the growth of macroscopic cluster aggregates.

PACS. 61.46.+w Clusters, nanoparticles, and nanocrystalline materials – 61.10.-i X-ray diffraction and scattering – 61.43.Hv Fractals; macroscopic aggregates

1 Introduction

In this decade, one big trend in the cluster science is the formation of new matters produced by accumulation of a great number of clusters. Recent researchers have prepared various sorts of macroscopic cluster aggregates with metallic or covalent bonding by using the neutral cluster deposition technique and have investigated some novel optical and magnetic properties [1, 2]. The internal structure and morphology of the macroscopic cluster aggregates depend on the coalescence and sintering processes. Usually, free metal clusters easily lose their specific conformations and internal structures during deposition, because they interfuse to grains in a granular state. The coalescence phenomena of clusters play an important role in determining structure of a nanometer range, which includes various local disorders such as grain boundary, twin boundary, dislocation, vacancy, and many other defects. One can anticipate that the physical and chemical properties are strongly affected by the degree of the coalescence growth. In order to control the local structure of the granular state, we need to study its growth feature.

The X-ray diffraction (XRD) method is very suitable to the study of the sintering of many clusters. Previous researchers have measured the growth of 20 nm Au powders with XRD [3]. However, the sintering of Au clusters smaller than 5 nm has hardly been observed, since such small clusters immediately coalesce during deposition or accumulation at room temperature [4]. To observe the sintering features of small Au clusters with XRD, we have constructed a novel apparatus with grazing-incidence X-ray diffraction (GIXRD) technique [5]. This apparatus enables us to prepare a great number of Au clusters on a cold substrate, where the clusters generated by the vapor-condensation method are quenched simultaneously with the deposition, in order that the coalescence may be avoided. Measurements can be done for the clusters deposited at low temperature and annealed at adequate higher temperatures. In this paper, we present *in situ* observation results of the coalescence growth taking place among 1–2 nm Au clusters.

2 Experiment

The apparatus is composed of a cluster formation chamber (FC), a deposition chamber (DC), and a GIXRD device, where the two chambers are connected with a nozzle. Clusters are generated in FC by the vapor condensation method with helium and carried into DC with a helium flow through a nozzle. The clusters are deposited on a cold substrate fixed to a liquid nitrogen cryostat placed in DC. After deposition, GIXRD measurements can be done for the sample without their exposure to the air. The details of the apparatus are described in our previous paper [5]. The experimental parameters for the generation of small Au clusters are 1498 K (source temperature), 2.7 kPa (helium

[a] *Current address:* National Institute of Materials and Chemical Research, 1-1 Higashi, Tsukuba, Ibaraki 305-8565, Japan

[b] e-mail: kkoga@home.nimc.go.jp

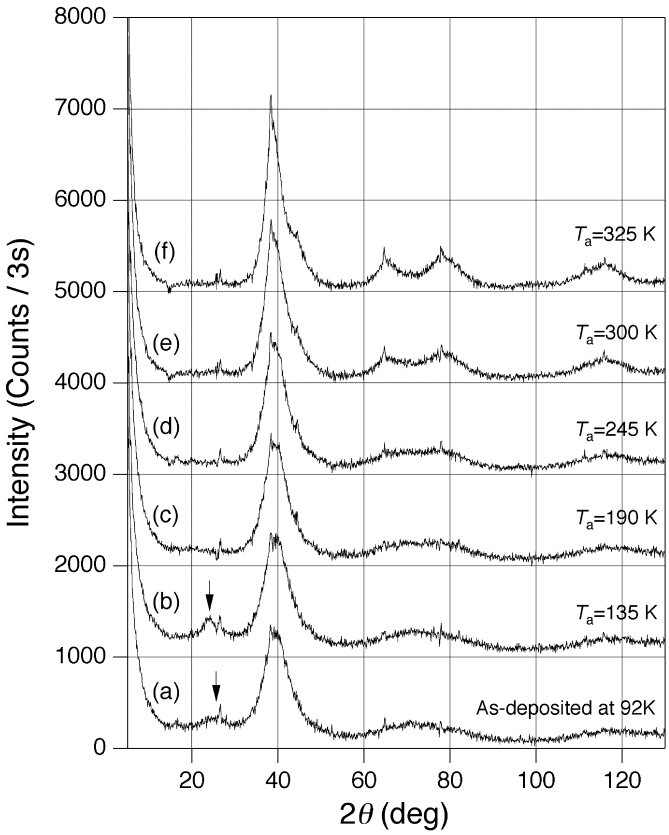

Fig. 1. Grazing-incidence X-ray diffraction patterns from (a) Au clusters deposited at 92 K, and after annealing at (b) 135 K, (c) 190 K, (d) 245 K, (e) 300 K, and (f) 325 K. All measurements were performed at 82 K. The broad peak denoted by an arrow comes from CO_2 molecules adsorbed on the cold Au clusters.

pressure of FC), 0.7 kPa (that of DC) and 15 mm (source–skimmer distance). Most of the generated Au clusters were found to have diameters of 1–2 nm. The size distribution of Au clusters could be well fitted by a log-normal function with a mean diameter 1.36 nm, full width at half maximum (FWHM) 1.16 nm, and the geometrical standard deviation 1.51.

A large number of Au clusters for building a macroscopic aggregate were deposited on a cooled Si(100) substrate at 92 K for 1 h. The GIXRD measurement was performed on the as-deposited sample at 82 K. Afterward, we heated the substrate up to an annealing temperature T_a, held it at T_a for 0.5 h, cooled it down to 82 K again, and performed the next measurement. The annealing procedures were done at $T_a = 135$, 190, 245, 300, and 325 K, in this order. The measured diffraction patterns are shown with solid lines in Fig. 1(a–f), where a background signal measured at 82 K before deposition was subtracted. The X-ray generator was operated under 50 kV and 300 mA. The Cu K_α characteristic X-rays diffracted from the sample were monochromatized with a highly oriented pyrolytic graphite crystal and detected by a scintillation counter. After collecting the last data shown in Fig. 1(f), the sample was transferred into the scanning electron microscope

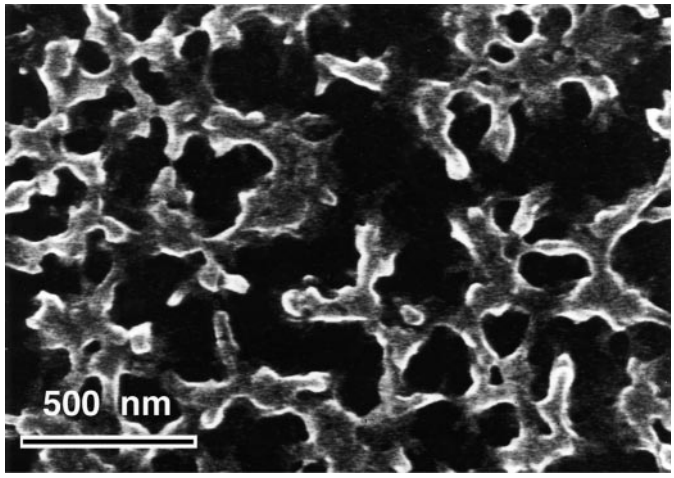

Fig. 2. A scanning electron microscope photograph of Au cluster aggregates formed by annealing the cold cluster deposit at 325 K. Lumpy-type networks with a typical size of 100 nm are developed over the macroscopic range.

(SEM) at room temperature under the air atmosphere. Figure 2 shows an SEM photograph taken under 3×10^4 magnification. The morphology shows the presence of a macroscopic network of lumps having a typical scale of 100 nm.

3 Analysis and discussion

A brief analysis of the diffraction pattern from the as-deposited state in Fig. 1(a) has already been done in our previous paper [6], in which the high resolution electron microscopic (HREM) observations were also performed. It was observed that larger clusters (2–3 nm) deposited sparsely on an amorphous carbon film showed the decahedral morphology very frequently. Our conclusion, drawn from both the diffraction pattern analysis and the HREM result, is that the as-deposited cold sample contained mainly decahedral-form clusters, with some structural imperfections, such as the inhomogeneous strains. The broad peak denoted by an arrow in Fig. 1(a) comes from contaminations which were trapped on the cooled substrate during the deposition. The peak around $2\theta = 25°$ originated from them was sharpened by annealing at 135 K, and disappeared after annealing at 190 K, as shown in Fig. 1(a–c). The pattern has started to change from $T_a = 190$ K due to the sublimation of contamination molecules separating Au clusters. We have judged that the contaminations are CO_2 because the sublimation temperature of CO_2 is 194.66 K. As the annealing temperature increases, the first peak sharpens and produces a small peak on the right shoulder, the second halo splits into two broad peaks, and the third halo becomes sharper and sharper.

We assumed at first that the experimental pattern of $T_a = 325$ K in Fig. 1(f) was coming from crystalline grain structures. Then the peak-separation procedures were done on this pattern using a nonlinear least-square fit-

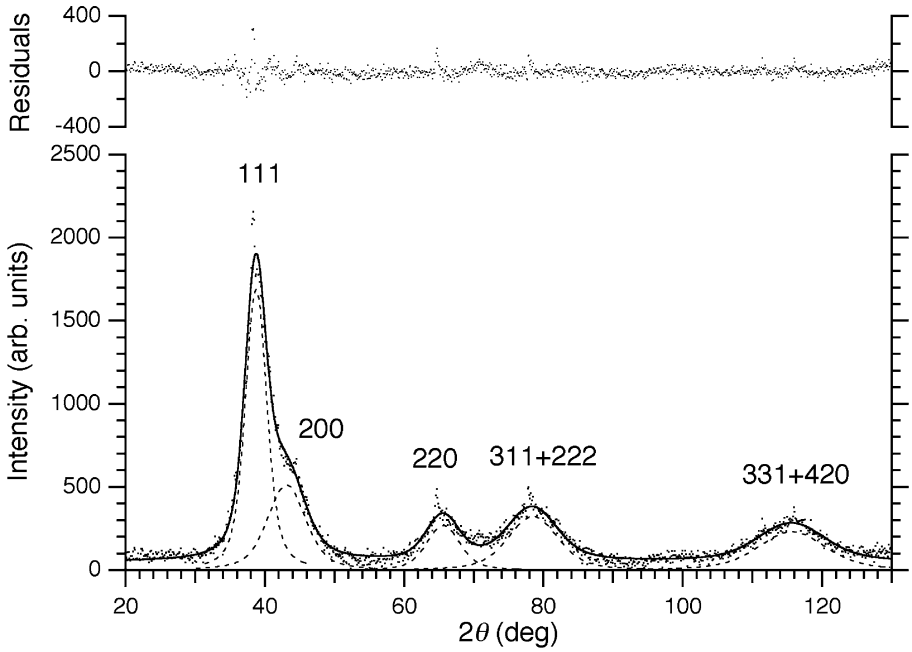

Fig. 3. The observed pattern from Au cluster aggregates after annealing at 325 K (dots) and nonlinear curve fitting results: total pattern (solid line) and separated peaks with Voigt functions (dashed line). Residuals between the observed and the fitting results are represented by dots.

ting package. A Voigt function with a common shape was used as a profile function, and five Voigt peaks were determined under a constant baseline. The fitting results are shown in Fig. 3. Assuming the face-centered cubic structure, fitted five peaks can be indexed to be 111, 200, 220, $311+222$, and $331+420$, as shown in Fig. 3, where 400 reflection around at $2\theta = 100°$ was too weak to be separated out. The determined peak positions, integrated intensities, and FWHM are tabulated in Table 1, along with values of the bulk Au. Mean grain sizes ε along $\langle 111 \rangle$, $\langle 100 \rangle$, and $\langle 110 \rangle$ directions were calculated by the application of the Sherrer equation to the first three peaks using the Sherrer constant of 0.9. These were also tabulated in Table 1. The coherent length along the $\langle 111 \rangle$ direction was determined to be 2.6 nm, corresponding to 11 stacking layers.

Next, tried to find out the most adequate crystalline model to represent the grain structures producing the diffraction pattern of T_a=325 K. The maximum coherent length was found to be along $\langle 111 \rangle$ directions. This implies that the representative grain structure has some (111) stacking faults weakening the X-ray coherence along $\langle 100 \rangle$ and $\langle 110 \rangle$ directions. Therefore, we first considered two kinds of models as the representative grain structure: spherical models having some (111) twinning faults, and cylindrical models elongated along $\langle 111 \rangle$ having some faults. The basic spherical model structure is the 5-shelled cuboctahedron having the same number of stacking layers as obtained by the peak separation analysis. We have introduced 1–4 lamella twinning planes into the 5-shelled cuboctahedron. The cylindrical models have 11 stacking planes, in which each plane has a hexagonal shape formed with 7, 19, or 37 atoms. We introduced 0–2 lamella twins into these models. However, not one of the spherical or cylindrical crystalline models with lamella twins could reproduce the whole experimental pattern at all.

Table 1. Peak positions ($2\theta_{exp}$), integrated intensities (I_{exp}), and full widths at half maximum (FWHM) of Bragg reflections obtained by the peak-separation procedure applied to the diffraction pattern of Fig. 1(f). The corresponding values of the bulk Au are present in parentheses. The average grain sizes ε along $\langle 111 \rangle$, $\langle 100 \rangle$, and $\langle 110 \rangle$ directions were calculated from the FWHM with the Sherrer equation. The length ξ is the maximum coherent length along $\langle 111 \rangle$, $\langle 100 \rangle$, and $\langle 110 \rangle$ directions in the 7-shelled decahedron.

hkl	$2\theta_{exp}$ ($2\theta_{bulk}$)	I_{exp} (I_{bulk})	FWHM	ε(nm)	ξ(nm)
111	38.7° (38.3°)	100 (100)	3.6°	2.6	3.3
200	43.1° (44.6°)	53.7 (49.3)	6.4°	1.4	1.4
220	65.6° (64.9°)	24.8 (32.8)	5.6°	1.8	2.0
$311+222$	78.4°	44.5 (51.0)			
$331+420$	115.6°	43.8 (47.4)			

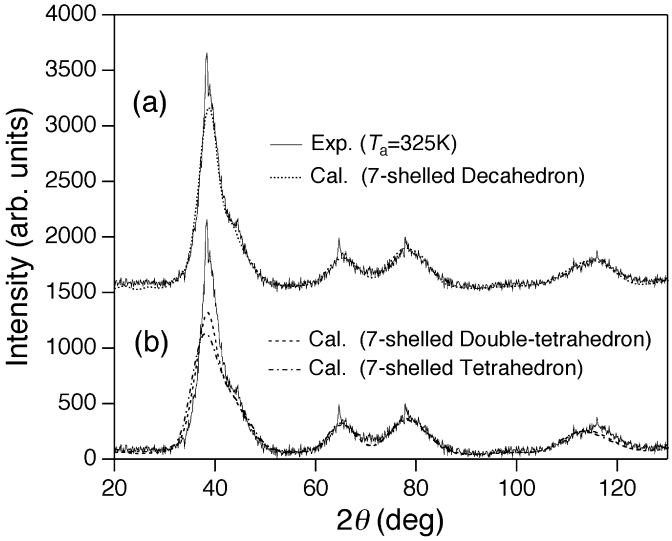

Fig. 4. The observed pattern from Au cluster aggregates after annealing at 325 K (solid line) and calculated patterns from (a) a geometric 7-shelled decahedral structure (dotted line), (b) a 7-shelled tetrahedral structure (dashed–dotted line), and a 7-shelled double-tetrahedral structure (dashed line).

Accordingly, we have considered the multiple-twinning decahedral models as the grain structure. The details of the decahedral structure model are described in [6]. Finally we could successfully reproduce the whole pattern using a geometric model of 7-shelled decahedron, as shown in Fig. 4(a). The Debye–Waller factor of the bulk Au at 94 K [7] was applied approximately to the calculated intensity. Figure 4(b) shows tests for fitting the experimental curve with either tetrahedra or double tetrahedra sharing two tetrahedra with a twin plane. The calculated intensities from these models show much disagreement with the experimental pattern, especially about the first peak. This indicates that the multiple-twinning relation of five tetrahedrons is essentially necessary to explain the observed pattern. Although the actual grains should not be represented with one structure model, because of some size distribution unknown at the present stage, we can say at least that the present successful profile reproduction suggests the presence of multiple-twinning grains. The maximum coherent lengths ξ along $\langle 111\rangle$, $\langle 100\rangle$, and $\langle 110\rangle$ directions in the 7-shelled decahedron are tabulated in Table 1 , where ξ along $\langle 111\rangle$ corresponds to the maximum length in a double tetrahedron shared in the decahedron, although each tetrahedral segment is deformed from the perfect crystal.

The peak-separation analysis results in Table 1, which were obtained by assuming crystalline grain structures, now have less physical meaning, since such an analysis can be applied only to the crystalline case. Nevertheless, the values of ξ were close to those of ε estimated from the peak widths. The broad peaks arising from such a large decahedral structure may be regarded as quasi-Bragg peaks, reflected from coherent regions in the structure. However, we refrain from further arguments on the tabulated results, because of the lack of a systematic study on widths of peaks from coherent lattice regions in the noncrystalline structure.

In Fig. 4(a), it can be seen that some additional small spikes were found at every crystalline Bragg peak position. These spikes arisen from $T_a = 245$ K, as seen in Fig. 1, are apparently from a small amount of large crystalline grains, which might be epitaxially grown on fewer initial crystalline clusters.

The final analysis suggests that the initial decahedral clusters coalesce to form nano-grain structures with multiple-twinning relations. The growth feature is therefore considered to be an epitaxial-like coalescence. Larger decahedral clusters existing in the cold as-deposited sample may work as seeds for producing multiple-twinned grain structures. The similar feature, that a large decahedral particle coalesced with another small particle grows into a new decahedral particle, has been observed in a previous *in situ* TEM observation [8]. Such a seed effect can take place because the coalescence event involves a neck formation followed by diffusion of surface atoms [9]. The growing rate, however, would be influenced by the amount of contamination among Au clusters. Although we have observed the sublimation of CO_2 at 190 K, the other contaminants, such as H_2O, remain possible even at 325 K. Therefore, we cannot treat the present slow growth feature as having an intrinsic nature. The lumps formed in the present experiment presumably include many vacancies and mesoscopic pores due to contaminant molecules. Nevertheless, the structural evolution observed here can be regarded as a specific feature of the sintering among Au clusters.

The authors wish to thank Mr. T. Ikeda of the University of Tsukuba for his helpful assistance in obtaining the experimental data.

References

1. J.P. Perez *et al.*: J. Magn. Magn. Mater. **145**, 74 (1995)
2. P. Melinon *et al.*: J. Chem. Phys. **107**, 10 278 (1997)
3. S. Iwama, T. Sahashi: Jpn. J. Appl. Phys. **19**, 1039 (1980)
4. J. Harada, K. Ohshima: Surf. Sci. **106**, 51 (1981)
5. K. Koga, H. Takeo: Rev. Sci. Instrum. **67**, 4092 (1996)
6. K. Koga, H. Takeo, T. Ikeda, K. Ohshima: Phys. Rev. B **57**, 4053 (1998)
7. C.H. Macgillavry, G.D. Rieck (Eds.): *International Tables for X-ray Crystallography* (D. Reidel Publishing Co., Netherlands 1983) vol. III, p.237
8. K. Yagi, K. Takayanagi, K. Kobayashi, G. Honjo: J. Cryst. Growth **28**, 117 (1975)
9. W. Krakow, M. Jóse-Yacamán, J.L. Aragón: Phys. Rev. B **49**, 10 591 (1994)